

Article

Zinc Oxide–Graphene Nanocomposite-Based Sensor for the Electrochemical Determination of Cetirizine

Rakesh R. Sawkar¹, Mahesh M. Shanbhag², Suresh M. Tuwar^{1,*}, Kunal Mondal^{3,4,*}  and Nagaraj P. Shetti^{5,6,*}¹ Department of Chemistry, Karnatak Science College, Dharwad 580001, Karnataka, India² Department of Chemistry, K.L.E. Institute of Technology, Hubballi 580027, Karnataka, India³ Idaho National Laboratory, Idaho Falls, ID 83415, USA⁴ Department of Civil & Environmental Engineering, Idaho State University, Pocatello, ID 83209, USA⁵ Department of Chemistry, School of Advanced Sciences, KLE Technological University, Vidyanagar, Hubballi 580031, Karnataka, India⁶ University Center for Research & Development (UCRD), Chandigarh University, Gharuan, Mohali 140413, Panjab, India

* Correspondence: tuwarsm@kscd.ac.in (S.M.T.); kunal.mondal@inl.gov (K.M.); dr.npshetti@gmail.com (N.P.S.)

Abstract: A nanocomposite electrode of graphene (Gr) and zinc oxide (ZnO) nanoparticles was fabricated to study the electrochemical oxidation behavior of an anti-inflammatory drug, i.e., cetirizine (CET). The voltametric response of CET for bare CPE, Gr/CPE, ZnO/CPE, and the ZnO-Gr nanocomposite electrode was studied. The modifier materials were characterized using scanning electron microscopy (SEM), energy-dispersive X-ray spectroscopy (EDS), and X-ray powder diffraction (XRD) to comprehend the surface morphology of the utilized modifiers. The influence of pH, scan rate, and accumulation time on the electrooxidation of CET was examined. It was found that the electrochemical oxidation of CET was diffusion-controlled, in which two protons and two electrons participated. The detection limit was found to be 2.8×10^{-8} M in a linearity range of 0.05–4.0 μ M. Study of excipients was also performed, and it was found that they had negligible interference with the peak potential of CET. The validation and utility of the fabricated nanocomposite sensor material were examined by analyzing clinical and biological samples. Stability testing of the nanocomposite electrode was conducted to assess the reproducibility, determining that the developed biosensor has good stability and high efficiency in producing reproducible results.

Keywords: cetirizine; graphene; zinc oxide nanoparticles; electrochemical oxidation; detection limit



Citation: Sawkar, R.R.; Shanbhag, M.M.; Tuwar, S.M.; Mondal, K.; Shetti, N.P. Zinc Oxide–Graphene Nanocomposite-Based Sensor for the Electrochemical Determination of Cetirizine. *Catalysts* **2022**, *12*, 1166. <https://doi.org/10.3390/catal12101166>

Academic Editors: Gopi Sivalingam, Kathiresan Murugavel and Kyusik Yun

Received: 6 September 2022

Accepted: 29 September 2022

Published: 3 October 2022

Publisher's Note: MDPI stays neutral with regard to jurisdictional claims in published maps and institutional affiliations.



Copyright: © 2022 by the authors. Licensee MDPI, Basel, Switzerland. This article is an open access article distributed under the terms and conditions of the Creative Commons Attribution (CC BY) license (<https://creativecommons.org/licenses/by/4.0/>).

1. Introduction

Cetirizine (CET) is a nonsteroidal anti-inflammatory drug (NSAID) and a second-generation antihistamine medication that has significant affinity with histamine H1 receptors [1,2]. CET's efficacy is demonstrated by its ability to prevent allergic reactions by inhibiting histamine activity in the body [3]. The presence of histamine in our bodies leads to allergic symptoms, including runny nose, sneezing, watery eyes, and itching [4]. CET can be employed in the treatment of allergic rhinitis and chronic urticaria. It can also be used as a medication for high fever and angioedema. CET is sold in the form of tablets, syrup, and oral drops under different brand names [5,6]. However, an overdose of CET can lead to mild drowsiness, fatigue, and headache [7]. Cetirizine hydrochloride has an average half-life of 8 h and has a long-acting metabolic effect. It can stay in the body for up to 20 h before getting excreted. Approximately 70% of CET is eliminated through urination, half of which is obtained as an unaltered cetirizine form. As a result, a sensitive method is necessary to trace the amount of CET in clinical and biological samples.

Numerous approaches have been tried for the determination of CET, including gas chromatography [8], calorimetry [9], high-performance liquid chromatography [10], potentiometry [11], electrophoresis [12], and some spectroscopic methods [9,13]. These techniques are costly, time-consuming, and require the preparation of an excessive quantity

of test samples. However, the voltametric approach has not been widely studied, despite its benefits of excellent selectivity, sensitivity, use of an apparently lower volume of analyte solution, rapid reaction time, and ease of handling [14]. However, bare electrodes exhibit some drawbacks in electrochemical processes, including slow electron transport and fouling [15]. These drawbacks can be resolved using sensitive and selective electrode materials with various modifications [16]. In recent years, chemical and biological sensors have significantly impacted medical examination, personal safety, and the environmental and agricultural fields [17–19]. However, the efficient operation of an electrochemical sensor mainly depends on the appropriate sensing material. The electrode must possess high stability, vast surface area, and high sensitivity [20,21]. In recent times, graphene and semiconductors have made a substantial contribution as suitable electrode modifiers in the fabrication of an efficient electrochemical sensor [22–24].

Graphene (Gr), a 2D material composed of a single atomic layer of carbon organized in a honeycomb lattice, has piqued the interest of a large number of scientists because of its exceptional properties. This 2D carbon allotrope has been widely predicted to have distinctive and novel uses in various applications. Due to its sp²-hybridized carbon and electronic assembly, it is the thinnest and strongest material and exhibits remarkable electrical, mechanical and thermal conductivity [25]. It is expected to be an ideal electrode material because of its essential qualities, such as superior property of electrical conductance, quick electron mobility, and a vast active surface area possessing good thermal and electrochemical features [26]. Given Gr's exceptional qualities, the advancement of graphene-based metal oxide composites is likely to be an innovative approach for an extensive range of applications, as it will produce composite electrodes with desired features [27]. Gr has a large specific area of 2630 m² g⁻¹ and can provide an excellent platform for constructing nanocomposites [28,29].

Zinc oxide (ZnO) is a semiconductor material with a significant excitation binding energy of 60 meV and a 3.37 eV wide band gap. ZnO is a favorable candidate for sensor applications due to its high catalytic proficiency, extraordinary electrical conductance, nontoxicity, and chemical stability [30]. ZnO has been extensively employed in the sensing field due to these unique properties [31,32]. Incorporating ZnO nanoparticles onto the graphene layers can enhance the surface area. It can display special, intriguing features because of the synergistic effect between ZnO and graphene, better electrical conductance, and improved electron transfer rate [33]. Electrochemical sensors based on graphene and metal oxide for detecting different chemical or biological molecules have been reported with promising results [34–37]. As per some published reports, Gr and ZnO nanocomposite were used in glucose sensing [38,39], gas sensing [40] and in detection of tyrosine [41] etc. The present method involves the synthesis of ZnO nanoparticles by precipitation. The ZnO was incorporated with graphene in carbon paste, which helped in the determination of cetirizine even in lower concentrations (50 nM), providing a low detection limit. Furthermore, the preparation method of ZnO nanoparticles and the electrode fabrication is economical, easy, and time-saving. The passivation problem of electrode can easily be removed by changing the paste and the removal of background current can be diminished by simple pretreatment. The electrode can produce reproducible signals. Thus, desired results are possible with the use of graphene and synthesized ZnO.

Hence, we fabricated a zinc oxide-incorporated graphene-modified carbon paste electrode (ZnO-Gr/CPE) to study the electrochemical nature of CET. The electrode developed showed excellent response, displaying an improved peak current compared with bare carbon paste electrode (CPE). The low detection limit value obtained showed that the electrode was highly sensitive. Interday and intraday measurements were carried out to check efficacy in terms of stability, and the data revealed the sensor could produce stable signals.

2. Results and Discussions

2.1. Characterization of Modifier

SEM-EDS was used for an elemental investigation of the ZnO-Gr modifier. Figure 1A,B display the SEM images obtained for ZnO-Gr, which shows the distribution of ZnO particles on the graphene surface. Figure 1C shows the EDS image of ZnO-Gr/CPE, with the distribution of the modifier. The composition of ZnO-Gr/CPE according to obtained EDS data was C 80.89%, O 17.77%, and Zn 1.34% (Table S1). The structural properties of the ZnO nanoparticles were revealed using powder X-ray diffraction (XRD) analysis. The XRD pattern of synthesized ZnO nanoparticles is shown in Figure 1D. This shows strong diffraction peaks at 31.7° , 34.4° , 36.2° , 47.5° , 56.6° , 62.8° , 66.3° , 67.9° , and 69.0° , corresponding to peak index (100), (002), (101), (102), (110), (103), (200), (112), and (201) reflection lines, respectively. All the peaks were confirmed a ZnO hexagonal phase (wurtzite structure) by comparison with JCPDS card number 01-080-3004. The sharp and narrow diffraction peaks indicated that the synthesized sample was crystalline in nature and small.

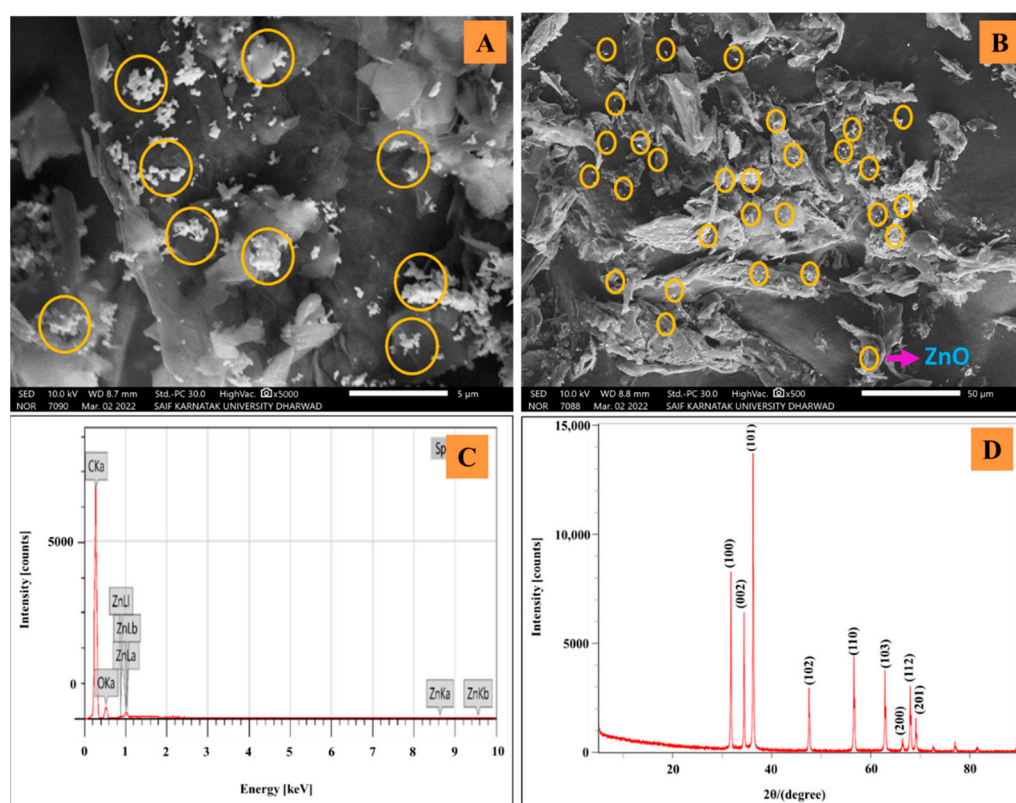


Figure 1. (A,B) SEM-EDS image of ZnO-Gr modifier, (C) EDS pattern of ZnO-Gr composite, (D) XRD pattern of ZnO nanoparticles.

2.2. Area of ZnO-Gr Sensor

The area of a working sensor plays a prominent role in electrochemical measurements as it directly induces the sensitivity of an electrode. Measurements were carried out to determine the area of ZnO-Gr using $K_3[Fe(CN)_6]$ (test solution) and 0.1 M KCl (supporting buffer). The CV measurements were documented for various scan rates, and then with the help of slope values obtained from the plot of peak current and $\nu^{1/2}$, the surface area was measured using the Randles–Sevcik Equation (1) [42]:

$$I_p = (2.69 \times 10^5) \times n^{3/2} \times A \times D_0^{1/2} \times \nu^{1/2} \times C \quad (1)$$

where I_p is peak current, n is the number of electrons transferred (1), A is area of electrode, D_0 is diffusion coefficient value ($7.6 \times 10^{-6} \text{ cm}^2 \text{ s}^{-1}$), C is concentration (0.001 M), and

the slope values for the plots of peak current (I_p) vs. square root of scan rate (\sqrt{v}) were found to be $33.56 \times 10^{-6} \text{ A}\cdot\text{M}^{-1}$ (bare CPE) and $70.68 \times 10^{-6} \text{ A}\cdot\text{M}^{-1}$ (ZnO-Gr/CPE). By calculation, the active surface area for bare CPE and ZnO-Gr/CPE, was 0.045 cm^2 and 0.0951 cm^2 , respectively.

2.3. Voltametric Behavior of CET

Electrochemical oxidation studies of CET were performed using cyclic voltammetry (CV). Cyclic voltammograms were recorded for bare carbon paste electrode (CPE), zinc oxide nanoparticle-modified CPE (ZnO/CPE), graphene-modified CPE (Gr/CPE), and zinc oxide and graphene-modified carbon paste electrode (ZnO-Gr/CPE) by immersing them in a glass cell containing 0.1 mM CET and PBS of pH 6.0. The voltametric responses of CET for different electrodes are displayed in Figure 2. The peak obtained at ZnO-Gr/CPE was found to be the maximum, with a peak current value of $20.12 \times 10^{-6} \text{ A}$. In the absence of an analyte molecule, no peaks were observed, and with the addition of CET, a single, sharp, well-oriented peak was observed in the forward scan. However, the highest peak current was displayed at ZnO-Gr/CPE due to the easy conductance of electrons towards the vicinity of the working electrode and the presence of enhanced surface area provided by the ZnO-Gr nanocomposite. The absence of a reduction in the backward scan indicates that the process is irreversible.

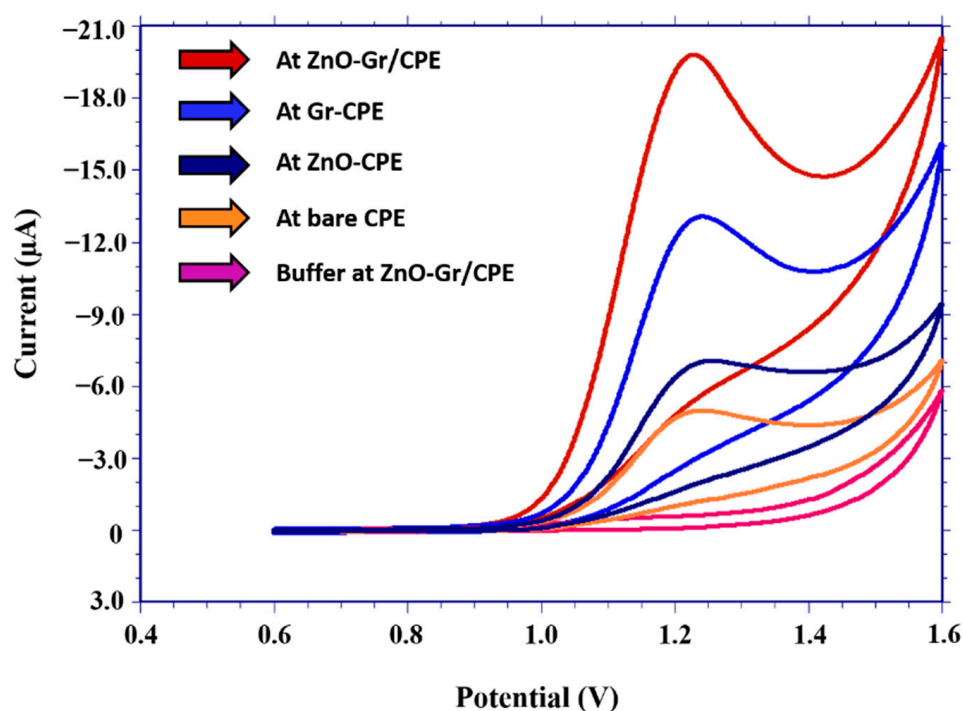


Figure 2. Cyclic voltammograms obtained for different electrodes for 0.1 mM CET in PBS of pH 6.0 at 0.05 V/s.

2.4. Accumulation Time

In voltametric measurements, the time required for the interaction between electrode and analyte molecules possesses a substantial role. The analyte molecule was driven towards the vicinity of the electrode by the concentration gradient of the analyte molecule, which may get adsorbed or diffused onto the surface of the electrode material, affecting the voltametric response. Hence, to study the accumulation time, the investigations were carried out for 0.1 mM CET at ZnO-Gr/CPE by varying the accumulation time from 0 to 70 s. We obtained different peak current values with the time variation (Figure 3). At 20 s of accumulation time, the peak obtained was sharp and well oriented, providing a maximum peak current, meaning that molecules were highly accumulated at the electrode's surface.

A saturation limit was reached below which the accumulation of molecules was hindered and displayed a lower peak current value of 30–70 s. Hence, the accumulation of 20 s was chosen for further measurements.

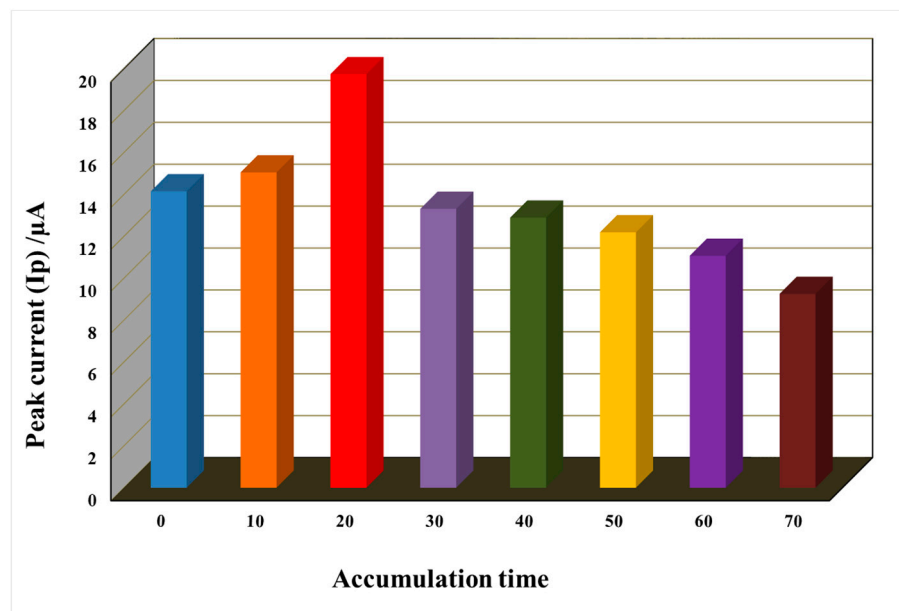


Figure 3. Effect of accumulation time on electrooxidation of CET.

2.5. pH Variation

In electrochemical investigations involving voltametric technique, the importance of supporting buffers is to assure considerable ionic strength of the solution, because in the process of oxidation and reduction of the analyte molecule, a homogeneous electric field must be maintained. The analyte response can be affected by the pH of the electrolyte. In this research, the response of CET in various pH solutions ranging from 3.0 to 11.2 was studied, and the respective cyclic voltammograms are shown in Figure 4A. It can be noticed that there was an increase in peak intensity of CET from pH 3.0 to pH 6.0 and later on, the peak current decreased. However, a well-defined peak was detected at pH 6.0 (Figure 4B), so was chosen for further investigations. The acidic constant (pKa) of CET is 8.0 and the ionic form of CET facilitates greater interaction with the electrode surface at pH 6.0–11.2 (nearer to the acidic constant of CET); hence, increased oxidation peaks were obtained at and above pH 6.0 [43]. The potential peak values of CET were shifted to less positive potential at pH 3.0–8.0. It became pH-independent, and from Figure 4C, it can be seen that the pH-independent peak potential displays a slope value of 8.7 mV/pH in the pH range from 8.0 to 11.2. The pH-dependent slope value of 44.8 mV/pH was observed between the pH range from 3.0 to 8.0, and the obtained value of slope was somewhat nearer the Nernstian value (59 mV/pH), implying the transfer of an equal number of protons and electrons [44] and the corresponding slope equation was specified as $E_p = 0.0448\text{pH} + 1.496$ $R^2 = 0.984$.

2.6. Scan Rate Effect

In voltametric measurements, scan rate study plays a significant role in understanding the analyte molecule's physicochemical characteristics. To study the scan rate effect, we opted for the CV technique, and the measurements were carried out for 0.1 mM CET in pH 6.0 of PBS by varying the scan rate from 0.05–0.30 V/s. The corresponding voltammograms are displayed in Figure 5A. It can be noticed that the peak current was increased when the scan rate was raised. Slight shifting of peak potential towards positive values was observed, which implies the process is irreversible [45], and the regression equation for peak current (I_p) and square root of scan rate (\sqrt{v}) is given as $I_p = 111.6 \sqrt{v} + 13.589$, $R^2 = 0.996$ (Figure 5B).

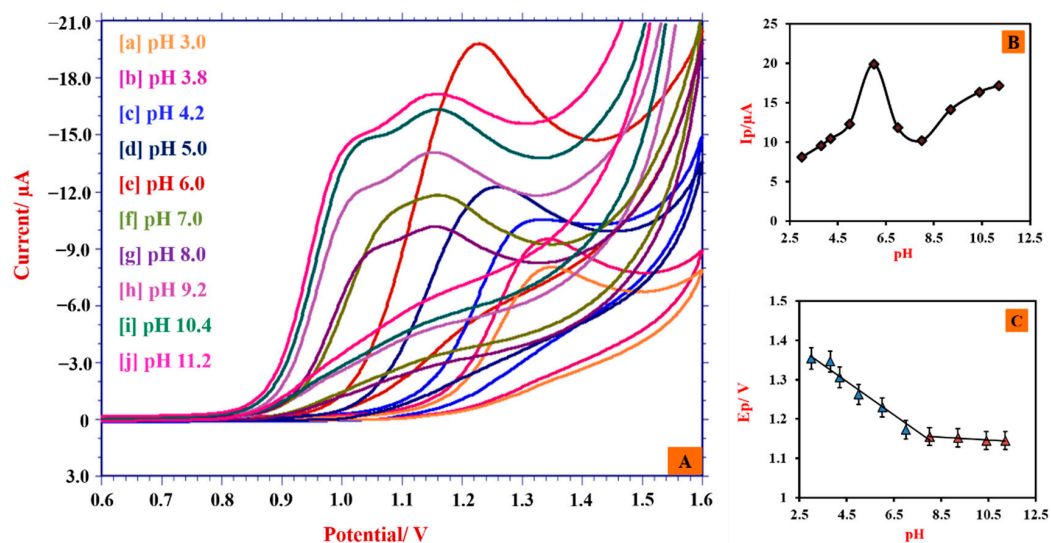


Figure 4. (A) Cyclic voltammograms observed for 0.1 mM CET in 0.2 M PBS of various pH solutions, (B) plots obtained for peak current (I_p) and pH, and (C) plots obtained for peak potential (E_p) and pH.

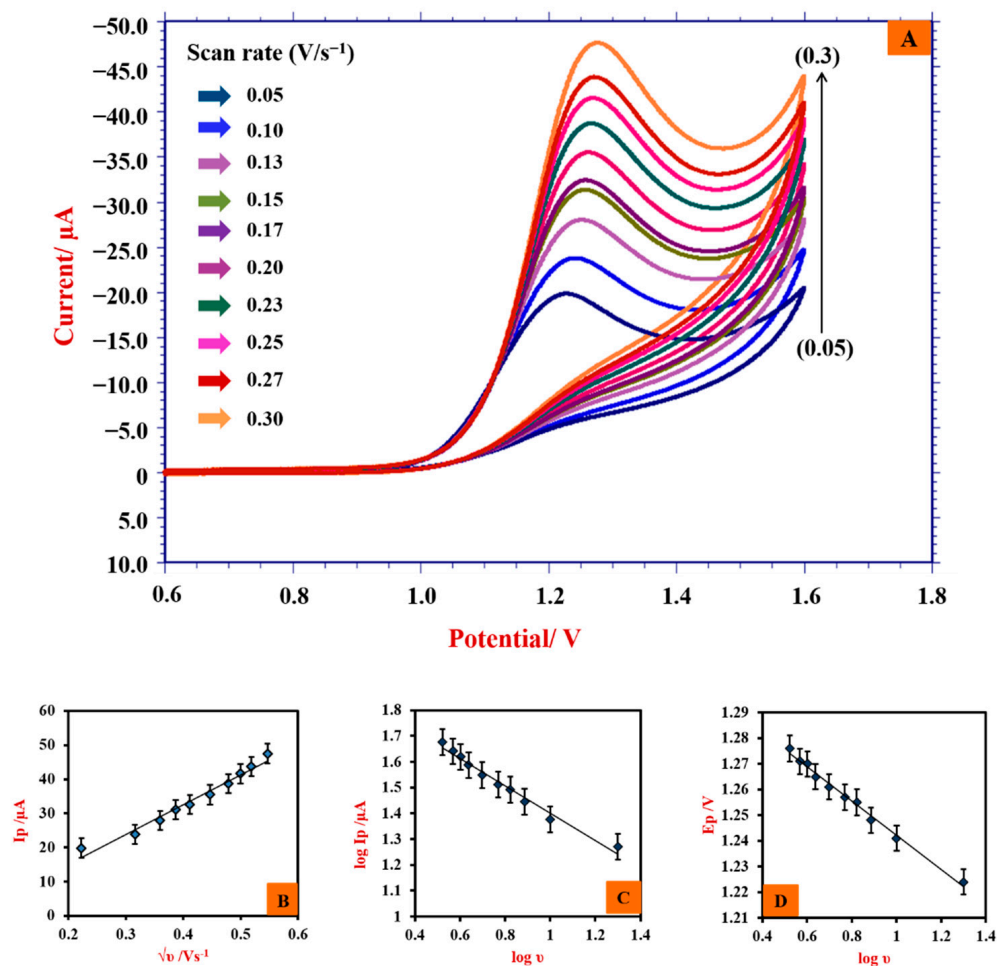


Figure 5. (A) Scan rate variation studies for 0.1 mM CET using PBS of pH 6.0 at ZnO-Gr/CPE with t_{imm} of 20 s. (B) Plot of peak current (I_p) vs. square root of scan rate (\sqrt{v}). (C) Dependence of log peak current ($\log I_p$) vs. log scan rate ($\log v$). (D) Plot of peak potential (E_p) vs. log scan rate ($\log v$).

The graph of log of peak current ($\log I_p$) vs. log scan rate ($\log v$) was plotted and obtained a linear regression equation $\log I_p = 0.5299 \log v + 1.9304$ $R^2 = 0.981$; Figure 5C.

The value of slope was in accordance with the standard value for the diffusion-controlled process (0.5) and hence the present system involves the process of diffusion [46].

Furthermore, the stoichiometry of electron transfer was determined using these scan rate studies. The plot of peak potential (E_p) vs. $\log v$ gives the linear regression equation $E_p = 0.0665 \log v + 1.3087$ $R^2 = 0.991$ Figure 5D. The slope value obtained was used to calculate the electron number.

For the system comprising irreversible electrode process, the Bard–Faulkner Equation (2) was used to estimate charge transfer coefficient (α) [47]; and the electrons transferred in the reaction (n) were calculated using Laviron's Equation (3) [48].

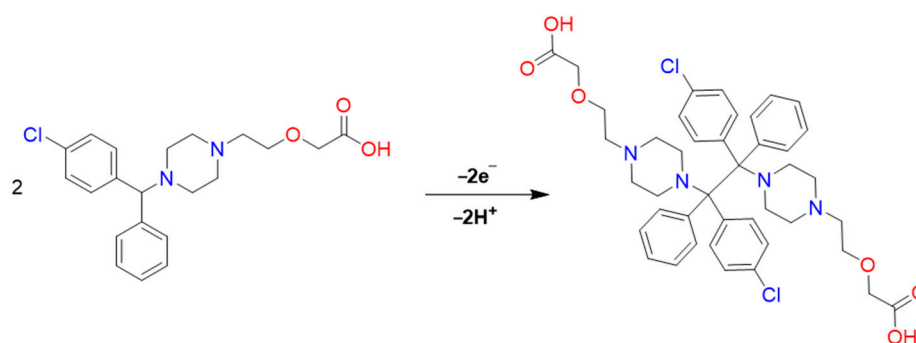
$$(E_p - E_{p/2}) = \Delta E_p = 47.7/\alpha \text{ (mV)} \quad (2)$$

$$E_p = K + [2.303RT/2(1 - \alpha)nF] \log v \quad (3)$$

In the above equation, α corresponds to the transfer coefficient, n is electron number, and the remaining notations represent their standard descriptions. By calculation, the electrons that participated during the electrooxidation process were found to be 1.79 (≈ 2), and α was found to be 0.59.

2.7. Possible Electrode Reaction

The electrooxidation of CET at ZnO-Gr/CPE was presumed to take place with the involvement of protons and by transferring an equal number of electrons and protons, as suggested by pH studies. The investigations of the scan rate revealed the number of electrons transferred in the reaction, which was calculated to be two. A possible mechanism is proposed using the above formulations, as depicted in Scheme 1 [3].



Scheme 1. Plausible electrooxidation of cetirizine.

3. Analytical Applications

3.1. Impact of Concentration

Differential pulse voltammetry (DPV) can provide sharp and well-defined peaks and help to determine analyte molecules even in the lowest analyte concentration; hence, we found DPV an appropriate technique to analyze CET quantitatively. The main objective of the concentration variation study is to know the concentration range at which the analyte molecule can be detected in the proposed sensor system and to estimate the detection limit. Hence, to investigate this, PBS of pH 6.0 has opted for quantification as a well-defined maximum peak current was observed at pH 6.0 (PBS) for ZnO-Gr/CPE. In the present study, the concentration of CET varied from 0.05 μM to 4 μM . These studies showed that the developed sensor can detect CET drugs in the lowest concentration range of 50 nM, proving the present investigation's significance. Further, it can be noticed from the Figure 6A that the increased concentration levels of CET caused peak current to increase gradually, giving the corresponding linearity equation: peak current (I_p) = 0.9435(C) + 0.742, $R^2 = 0.982$

(Figure 6B). This equation provides the slope and intercept value by which the detection limit and quantification limit was estimated using Equations (4) and (5) [49].

$$D_L = 3 \times s/m \quad (4)$$

$$Q_L = 10 \times s/m \quad (5)$$

where s represents standard deviation and m represents the slope value of the calibration plot. D_L and Q_L were computed to be 2.8×10^{-8} M and 9.1×10^{-8} M, respectively, for the ZnO-Gr electrode system. Further, the obtained D_L was compared with some of the voltammetric techniques used in determining CET involving different electrode systems, shown in Table 1. Due to the good electrical conductivity of graphene and good electroactive property of ZnO. Further, Gr possesses a unique structure with excellent electronic properties, e.g., being ultrathin and having a large specific surface area, extremely high electron mobility, and high sensitivity to electronic perturbations [50]. ZnO's high surface/volume ratio, surface tailoring ability, novel electron transport properties, and electronic conductance multifunctionality mean it is possible to detect a biomolecule at a lower concentration [51]. Hence, a promising sensing platform with good sensitivity along with low detection limit was obtained with ZnO-Gr/CPE.

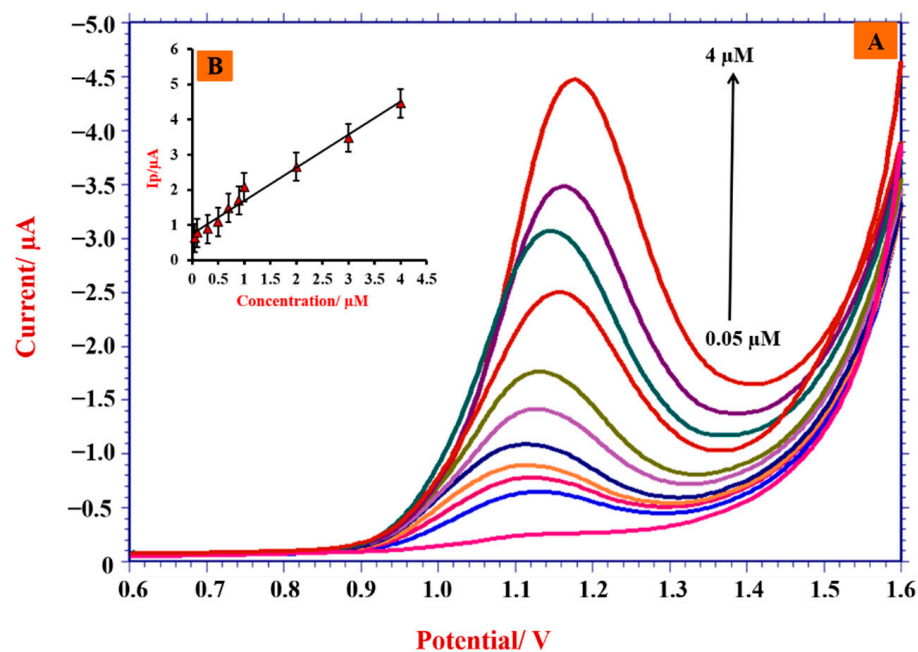


Figure 6. (A) Differential pulse voltammograms obtained for different concentrations of CET at ZnO-Gr/CPE using PBS of pH 6.0. (B) Plot of peak current (I_p) vs. CET concentration (C).

Table 1. Comparative study with earlier reports.

Electrode Used	Detection Limit (M)	Reference
GCE/MWCNT	7.1×10^{-6}	[52]
GCE	4.3×10^{-6}	[53]
Pretreated PGE	0.2×10^{-6}	[54]
Spectrophotometric determination	2.4×10^{-7}	[55]
BDD film electrode	1.6×10^{-8}	[56]
MWCNT-PtNPs/CPE	5.8×10^{-8}	[2]
ZnO-Gr/CPE	2.8×10^{-8}	Present method

Abbreviations: GCE—glassy carbon electrode, MWCNT—multiwalled carbon nanotube, PGE—pencil graphite electrode, BDD—boron-doped diamond, PtNPs—platinum nanoparticles, CPE—carbon paste electrode, ZnO-Gr—zinc oxide and graphene nanocomposite-modified carbon paste electrode.

3.2. Excipient Interference Study

In the formulation of a pharmaceutical drug, excipients play a pivotal role. An excipient is a substance added to the main content of a drug comprising a solid formulation with a potent active ingredient in minimal amounts for long-term stabilization. CET was determined at the ZnO-Gr/CPE to verify the sensor's selectivity in the presence of various excipients utilized in the drug formulation. This study included some of the commonly used pharmaceutical excipients. The excipients used and their response toward the peak potential value of CET was displayed in Figure 7.

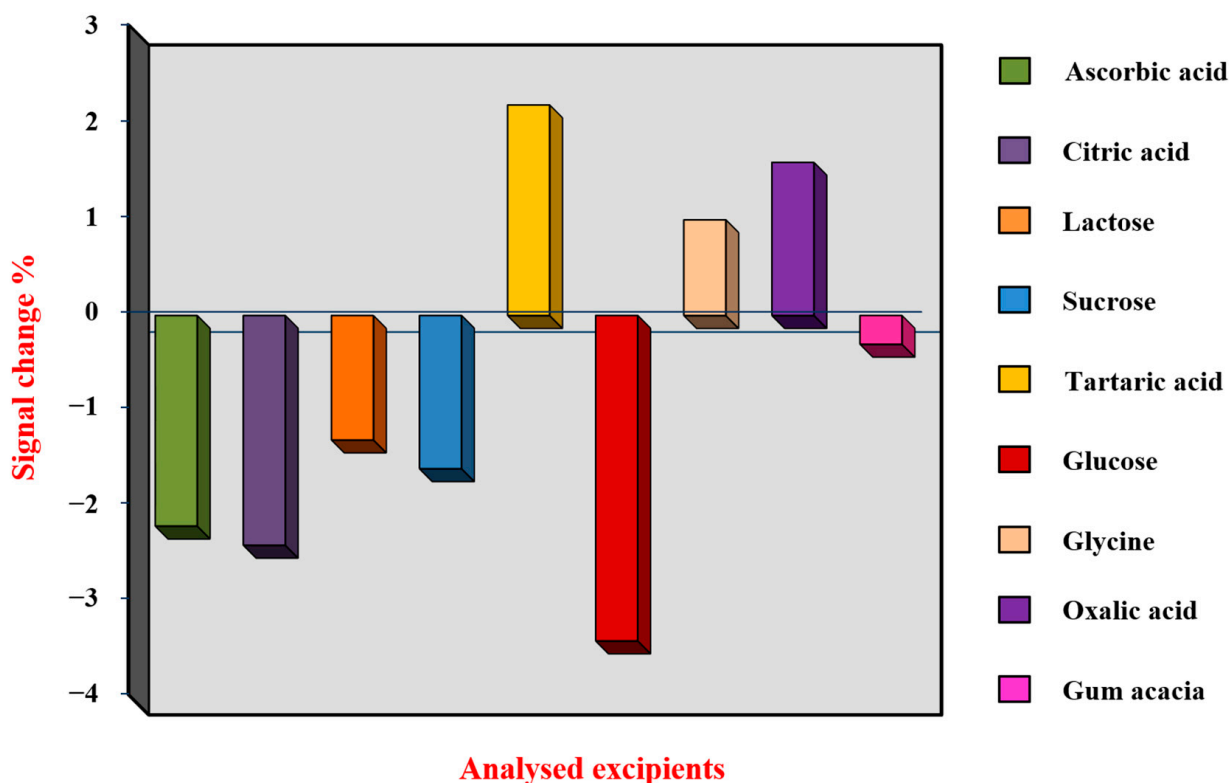


Figure 7. Analysis of excipients.

3.3. Tablet Sample Analysis

The method developed was employed to study the sensor's practical applicability in determining CET in pharmaceutical and urine samples. For pharmaceutical sample analysis, a commercially available CET tablet was used. The tablets were ground to form a powder, the powder was mixed in Millipore water, and a stock solution was prepared, as mentioned in Section 2.4. A sample concentration was taken and analyzed using DPV, and the results are displayed in Table 2. The recovery obtained agreed with the labeled claim, proving the proposed sensor's efficacy.

Table 2. Analysis of pharmaceutical sample.

Cetirizine	Observations
Amount specified (mg)	10
Amount obtained (mg) ^a	9.69
RSD %	3.69%
Added (mg)	1
Obtained (mg) ^a	0.86
Recovery	96.92%

^a Average of three replicate measurements.

3.4. Urine Sample Analysis

For cetirizine 10 mg tablets, mean peak plasma concentration (C_{max}) is 311 ng/mL. Mainly eliminated in the urine, between 70% and 85% (approximately 0.020 μ M) of an orally administered dose is found in the urine and 10% to 13% in the feces [57]. The developed electrode's reliability was demonstrated by the analysis of urine sample assay carried out under ideal conditions. The samples were prepared as mentioned in Section 2.4. The known concentration of CET was spiked to a urine sample and analyzed. The recovery obtained was determined using a plot obtained from concentration variation studies. The recovery range obtained in Table 3 suggests that the ZnO-Gr/CPE can efficiently determine CET in real samples.

Table 3. Determination of CET in urine samples.

Sample	Spiked (10^{-6} M)	Found (10^{-6} M)	Recovery %
1	1.0	0.99	99.8
2	2.0	1.92	96.4
3	3.0	2.78	92.7

3.5. Stability of the Sensor

The repeatability nature of the proposed sensor was validated by taking intraday measurements at regular intervals. A known CET concentration in PBS at pH 6.0 was used as a test solution and analyzed using the CV technique at this system's standard scan rate, i.e., 0.05 V/s at ZnO-Gr/CPE. It can be concluded from our observations that excellent repeatability was observed with an RSD% of 3.12 (Figure S2A). To study the reproducibility of the proposed sensor, the electrode was fabricated as described in Section 2.5 and kept in an air-sealed container for 10 days. Measurements were taken for preanalyzed concentrations of CET, maintaining optimum conditions (Figure S2B). The results proved that the modified electrode could produce reproducible results, as the peak current retained 95.4% of its original peak current value. This demonstrated the excellent reproducibility and repeatability of the developed ZnO-Gr/CPE sensor.

4. Experimental

4.1. Materials and Reagents

All the investigations were carried out using analytical-grade reagents. Cetirizine and graphene were obtained from Sigma-Aldrich. ZnO was prepared by coprecipitation. The chemicals required for preparing phosphate buffer solution (PBS) and preparation of ZnO nanoparticles were procured from Molychem Pvt Ltd. PBS was prepared for different pH levels using a suitable quantity of KH_2PO_4 , Na_2HPO_4 , and H_3PO_4 .

4.2. Instrumentation

Investigations of pH were performed employing a pH meter (Equiptronics). For voltammetric measurements, an electrochemical analyzer (CHI 1112C) was employed consisting of a three-electrode compartment in a glass cell with a counter electrode (Platinum), working electrode (ZnO-Gr/CPE), and reference electrode (Ag/AgCl). Surface characteristics studies were exploited using scanning electron microscopy with energy-dispersive spectroscopy (SEM-EDS, Jeol), and XRD (Smartlab SE, Rigaku, Tokyo, Japan) was employed to study the crystallinity of the ZnO nanoparticles.

4.3. Synthesis of ZnO Nanoparticles

The synthesis of zinc oxide nanoparticles was carried out as per literature [58]. In short, the procedure involves dissolving 0.2 M of zinc acetate in 50 mL of a solvent comprising an equal volume of ethanol and Millipore water, followed by the dropwise addition of potassium hydroxide (0.4 M). This mixture was stirred for 3 h in a magnetic stirrer at 80 °C until a white precipitate was obtained. The homogeneous mix containing white suspension

was centrifuged at 5000 rpm for about 30 min. The supernatant liquid was discarded, and the liquid with white residue was obtained. It was then collected and kept in a hot oven for drying, maintaining 120 °C until a powder form was obtained. This was followed by calcination for 3 h at 500 °C. The obtained ZnO nanopowder was characterized using XRD and SEM analysis.

4.4. Tablet and Urine Sample Preparation

CET tablets were procured from a local pharmacy under the brand name Cetzine. The tablets were finely powdered in a mortar. Weight corresponding to 1.0 mM CET was weighed and dissolved in Millipore water, followed by sonication for complete dissolution. A known concentration of the tablet sample was taken and analyzed employing the differential pulse voltametric (DPV) approach.

For recovery studies, urine samples were obtained from healthy individuals and diluted with an electrolytic solution of pH 6.0. A known CET concentration was spiked in urine samples, and recovery investigations were recorded. The CET concentration in the urine samples was determined using a calibration curve.

4.5. Fabrication of ZnO-Gr/CPE

The bare CPE was fabricated by mixing graphite powder and minerals (7:3) using a mortar and pestle. The paste was loaded into the cavity of a Teflon tube with a copper rod for electrical conductivity. The electrode was then smoothed on a polished surface and washed with Millipore water. The preparation of ZnO-Gr involved the same procedure, where Gr (0.05 g) and ZnO nanoparticles (0.05 g) were added, along with graphite and mineral oil. After the fabrication, the electrode was subjected to pretreatment to minimize the background current, which was done by scanning a CV using PBS of pH 6.0 at a scan rate of 0.5 V/s for 20 cycles. After every measurement, the paste was discarded from the electrode cavity, which was then loaded with new paste.

5. Conclusions

The electrochemical oxidation of CET was investigated by a nanocomposite electrode fabricated with graphene and zinc oxide nanoparticles. ZnO nanoparticles were prepared by coprecipitation and characterized by XRD. The electrochemical process in the present study was found to be irreversible, displaying a single sharp oxidation peak at ZnO-Gr/CPE. The oxidation process was observed to be pH-dependent and diffusion-controlled with the involvement of an equal number of protons and electrons in the reaction. A possible reaction mechanism was proposed. The quantification study proved that the linearity range and detection limit were comparable to reported methods. Real samples were analyzed to assess the practical applicability of the conventional sensor in pharmaceuticals. An interference study investigated the effect of some commonly used clinical excipients. Finally, the validation of ZnO-Gr/CPE was achieved by examining the stability of the electrode.

Supplementary Materials: The following supporting information can be downloaded at: <https://www.mdpi.com/article/10.3390/catal12101166/s1>, Figure S1: Graphical abstract of electrochemical oxidation of CET with ZnO-Gr/CPE; Figure S2: (A) Repeatability of ZnO-Gr/CPE, (B) Reproducibility of ZnO-Gr/CPE; Table S1: EDS of ZnO-Gr/CPE.

Author Contributions: Conceptualization, R.R.S., M.M.S., S.M.T., K.M. and N.P.S.; methodology, R.R.S., M.M.S. and S.M.T.; formal analysis, R.R.S. and M.M.S.; investigation, R.R.S., M.M.S., S.M.T., K.M. and N.P.S.; resources, S.M.T. and N.P.S.; data curation, R.R.S., M.M.S., S.M.T. and N.P.S.; writing—original draft preparation, R.R.S., M.M.S., S.M.T., K.M. and N.P.S.; writing—review and editing, R.R.S., M.M.S., S.M.T., K.M. and N.P.S.; supervision, S.M.T., K.M. and N.P.S. All authors have read and agreed to the published version of the manuscript.

Funding: This research received no external funding.

Institutional Review Board Statement: The institutional approval reference is INL/JOU-22-69018.

Informed Consent Statement: Not applicable.

Data Availability Statement: Not applicable.

Acknowledgments: The authors are thankful to USIC, Karnatak University, Dharwad for SEM-EDS and XRD analysis. Kunal Mondal gratefully acknowledges the Department of Energy and Environment Science and Technology at the Idaho National Laboratory, USA for their support.

Conflicts of Interest: The authors declare no conflict of interest.

References

1. Rudaz, S.; Souverain, S.; Schelling, C.; Deleers, M.; Klomp, A.; Norris, A.; Vu, T.; Ariano, B.; Veuthey, J.-L. Development and validation of a heart-cutting liquid chromatography–mass spectrometry method for the determination of process-related substances in cetirizine tablets. *Anal. Chim. Acta* **2003**, *492*, 271–282. [[CrossRef](#)]
2. Kalambate, P.K.; Srivastava, A.K. Simultaneous voltammetric determination of paracetamol, cetirizine and phenylephrine using a multiwalled carbon nanotube-platinum nanoparticles nanocomposite modified carbon paste electrode. *Sens. Actuators B Chem.* **2016**, *233*, 237–248. [[CrossRef](#)]
3. Vernekar, P.R.; Shetti, N.P.; Shanbhag, M.M.; Malode, S.J.; Malladi, R.S.; Reddy, K.R. Novel layered structured bentonite clay-based electrodes for electrochemical sensor applications. *Microchem. J.* **2020**, *159*, 105441. [[CrossRef](#)]
4. Kudchi, R.S.; Shetti, N.P.; Malode, S.J.; Todakar, A.B. Electroanalysis of an antihistamine drug at nano structured modified electrode. *Mater. Today Proc.* **2019**, *18*, 558–565. [[CrossRef](#)]
5. Kowalski, P.; Plenis, A. Comparison of HPLC and CE methods for the determination of cetirizine dihydrochloride in human plasma samples. *Biomed. Chromatogr.* **2007**, *21*, 903–911.
6. Einarson, A.; Bailey, B.; Jung, G.; Spizzirri, D.; Baillie, M.; Koren, G. Prospective controlled study of hydroxyzine and cetirizine in pregnancy. *Ann. Allergy Asthma Immunol.* **1997**, *78*, 183–186.
7. Pagliara, A.; Testa, B.; Carrupt, P.-A.; Jolliet, P.; Morin, C.; Morin, D.; Urien, S.; Tillement, J.-P.; Rihoux, J.-P. Molecular properties and pharmacokinetic behavior of cetirizine, a zwitterionic H1-receptor antagonist. *J. Med. Chem.* **1998**, *41*, 853–863. [[CrossRef](#)]
8. Baltés, E.; Coupez, R.; Brouwers, L.; Gobert, J. Gas chromatographic method for the determination of cetirizine in plasma. *J. Chromatogr. B Biomed. Sci. Appl.* **1988**, *430*, 149–155. [[CrossRef](#)]
9. Gazy, A.A.; Mahgoub, H.; El-Yazbi, F.; El-Sayed, M.; Youssef, R.M. Determination of some histamine H1-receptor antagonists in dosage forms. *J. Pharm. Biomed. Anal.* **2002**, *30*, 859–867. [[CrossRef](#)]
10. Jaber, A.; Al Sherife, H.; Al Omari, M.; Badwan, A. Determination of cetirizine dihydrochloride, related impurities and preservatives in oral solution and tablet dosage forms using HPLC. *J. Pharm. Biomed. Anal.* **2004**, *36*, 341–350. [[CrossRef](#)]
11. Rizk, N.M.; Abbas, S.S.; El-Sayed, F.A.; Abo-Bakr, A. Novel ionophore for the potentiometric determination of cetirizine hydrochloride in pharmaceutical formulations and human urine. *Int. J. Electrochem. Sci.* **2009**, *4*, 396–406.
12. Marák, J.; Staňová, A. Buffer salt effects in off-line coupling of capillary electrophoresis and mass spectrometry. *Electrophoresis* **2014**, *35*, 1268–1274. [[CrossRef](#)] [[PubMed](#)]
13. Gowda, B.; Melwanki, M.; Seetharamappa, J. Extractive spectrophotometric determination of ceterizine HCl in pharmaceutical preparations. *J. Pharm. Biomed. Anal.* **2001**, *25*, 1021–1026. [[CrossRef](#)]
14. Bukkitgar, S.D.; Shetti, N.P.; Malladi, R.S.; Reddy, K.R.; Kalanur, S.S.; Aminabhavi, T.M. Novel ruthenium doped TiO₂/reduced graphene oxide hybrid as highly selective sensor for the determination of ambroxol. *J. Mol. Liq.* **2020**, *300*, 112368. [[CrossRef](#)]
15. Sawkar, R.R.; Shanbhag, M.M.; Tuwar, S.M.; Shetti, N.P. Silica gel-based electrochemical sensor for tinidazole. *Sens. Int.* **2022**, *3*, 100192. [[CrossRef](#)]
16. Vernekar, P.R.; Shanbhag, M.M.; Shetti, N.P.; Mascarenhas, R.J. Silica-gel incorporated carbon paste sensor for the electrocatalytic oxidation of famotidine and its application in biological sample analysis. *Electrochem. Sci. Adv.* **2021**, e2100093. [[CrossRef](#)]
17. Sawkar, R.R.; Patil, V.B.; Tuwar, S.M. Electrochemical oxidation of atorvastatin using graphene oxide and surfactant-based sensor. *Mater. Today Proc.* **2022**; in press. [[CrossRef](#)]
18. Shanbhag, M.M.; Shetti, N.P.; Kalanur, S.S.; Pollet, B.G.; Nadagouda, M.N.; Aminabhavi, T.M. Hafnium doped tungsten oxide intercalated carbon matrix for electrochemical detection of perfluorooctanoic acid. *Chem. Eng. J.* **2022**, *434*, 134700. [[CrossRef](#)]
19. Shetti, N.P.; Malode, S.J.; Ilager, D.; Reddy, K.R.; Shukla, S.S.; Aminabhavi, T.M. A novel electrochemical sensor for detection of molinate using ZnO nanoparticles loaded carbon electrode. *Electroanalysis* **2019**, *31*, 1040–1049. [[CrossRef](#)]
20. Erady, V.; Mascarenhas, R.J.; Satpati, A.K.; Detriche, S.; Mekhalif, Z.; Delhalle, J.; Dhason, A. A novel and sensitive hexadecyltrimethylammoniumbromide functionalized Fe decorated MWCNTs modified carbon paste electrode for the selective determination of Quercetin. *Mater. Sci. Eng. C* **2017**, *76*, 114–122. [[CrossRef](#)]
21. Patil, V.B.; Sawkar, R.R.; Tuwar, S.M. Electrochemical oxidation of ketorolac at graphene oxide-based sensor. *Mat. Today Proc.* **2022**; in press. [[CrossRef](#)]
22. Jain, R. Voltammetric determination of cefpirome at multiwalled carbon nanotube modified glassy carbon sensor-based electrode in bulk form and pharmaceutical formulation. *Colloids Surf. B Biointerfaces* **2011**, *87*, 423–426. [[CrossRef](#)]
23. Kang, C.G.; Kang, J.W.; Lee, S.K.; Lee, S.Y.; Cho, C.H.; Hwang, H.J.; Lee, Y.G.; Heo, J.; Chung, H.-J.; Yang, H. Characteristics of CVD graphene nanoribbon formed by a ZnO nanowire hardmask. *Nanotechnology* **2011**, *22*, 295201. [[CrossRef](#)] [[PubMed](#)]

24. Wang, J.; Li, Y.; Ge, J.; Zhang, B.-P.; Wan, W. Improving photocatalytic performance of ZnO via synergistic effects of Ag nanoparticles and graphene quantum dots. *Phys. Chem. Chem. Phys.* **2015**, *17*, 18645–18652. [[CrossRef](#)]
25. Soldano, C.; Mahmood, A.; Dujardin, E. Production, properties and potential of graphene. *Carbon* **2010**, *48*, 2127–2150. [[CrossRef](#)]
26. Pumera, M. Graphene in biosensing. *Mater. Today* **2011**, *14*, 308–315. [[CrossRef](#)]
27. Low, S.S.; Tan, M.T.; Loh, H.-S.; Khiew, P.S.; Chiu, W.S. Facile hydrothermal growth graphene/ZnO nanocomposite for development of enhanced biosensor. *Anal. Chim. Acta* **2016**, *903*, 131–141. [[CrossRef](#)]
28. Yazid, S.N.A.M.; Isa, I.M.; Bakar, S.A.; Hashim, N.; Ghani, S.A. A review of glucose biosensors based on graphene/metal oxide nanomaterials. *Anal. Lett.* **2014**, *47*, 1821–1834. [[CrossRef](#)]
29. Zhang, D.; Ashraf, M.A.; Liu, Z.; Li, C.; Peng, W. Effect of graphene nanoplatelets addition on the elastic properties of short ceramic fiber-reinforced aluminum-based hybrid nanocomposites. *Mech. Based Des. Struct. Mach.* **2022**, *50*, 1417–1433. [[CrossRef](#)]
30. Lu, J.; Ng, K.M.; Yang, S. Efficient, one-step mechanochemical process for the synthesis of ZnO nanoparticles. *Ind. Eng. Chem. Res.* **2008**, *47*, 1095–1101. [[CrossRef](#)]
31. Ahmad, R.; Tripathy, N.; Jang, N.K.; Khang, G.; Hahn, Y.-B. Fabrication of highly sensitive uric acid biosensor based on directly grown ZnO nanosheets on electrode surface. *Sens. Actuators B Chem.* **2015**, *206*, 146–151. [[CrossRef](#)]
32. Jacobs, M.; Muthukumar, S.; Selvam, A.P.; Craven, J.E.; Prasad, S. Ultra-sensitive electrical immunoassay biosensors using nanotextured zinc oxide thin films on printed circuit board platforms. *Biosens. Bioelectron.* **2014**, *55*, 7–13. [[CrossRef](#)]
33. Low, S.S.; Loh, H.-S.; Boey, J.S.; Khiew, P.S.; Chiu, W.S.; Tan, M.T. Sensitivity enhancement of graphene/zinc oxide nanocomposite-based electrochemical impedance genosensor for single stranded RNA detection. *Biosens. Bioelectron.* **2017**, *94*, 365–373. [[CrossRef](#)] [[PubMed](#)]
34. Chen, X.; Yan, H.; Shi, Z.; Feng, Y.; Li, J.; Lin, Q.; Wang, X.; Sun, W. A novel biosensor based on electro-co-deposition of sodium alginate-Fe₃O₄-graphene composite on the carbon ionic liquid electrode for the direct electrochemistry and electrocatalysis of myoglobin. *Polym. Bull.* **2017**, *74*, 75–90. [[CrossRef](#)]
35. Liu, J.; Cui, M.; Niu, L.; Zhou, H.; Zhang, S. Enhanced peroxidase-like properties of graphene–hemin-composite decorated with Au nanoflowers as electrochemical aptamer biosensor for the detection of K562 leukemia cancer cells. *Chem. A Eur. J.* **2016**, *22*, 18001–18008. [[CrossRef](#)] [[PubMed](#)]
36. Patil, V.B.; Malode, S.J.; Mangasuli, S.N.; Tuwar, S.M.; Mondal, K.; Shetti, N.P. An electrochemical electrode to detect theophylline based on copper oxide nanoparticles composited with graphene oxide. *Micromachines* **2022**, *13*, 1166. [[CrossRef](#)] [[PubMed](#)]
37. Salihi, E.; Mekawy, M.; Hassan, R.Y.; El-Sherbiny, I.M. Synthesis, characterization and electrochemical-sensor applications of zinc oxide/graphene oxide nanocomposite. *J. Nanostructure Chem.* **2016**, *6*, 137–144. [[CrossRef](#)]
38. Zang, J.; Li, C.M.; Cui, X.; Wang, J.; Sun, X.; Dong, H.; Sun, C.Q. Tailoring zinc oxide nanowires for high performance amperometric glucose sensor. *Electroanalysis* **2007**, *19*, 1008–1014. [[CrossRef](#)]
39. Zhang, F.F.; Wang, X.; Ai, S.; Sun, Z.; Wan, Q.; Zhu, Z.; Xia, Y.; Jin, L.; Yamamoto, K. Immobilization of uricase on ZnO nanorods for a reagentless uric acid biosensor. *Anal. Chim. Acta* **2004**, *519*, 155–160. [[CrossRef](#)]
40. Xia, Y.; Li, R.; Chen, R.; Wang, J.; Xiang, L. 3D Architected Graphene/Metal Oxide Hybrids for Gas Sensors: A Review. *Sensors* **2018**, *18*, 1456. [[CrossRef](#)]
41. Norouz, P.; Salimi, H.; Tajik, S.; Beitollahi, H.; Rezapour, M.; Larijani, B. Biosensing Applications of ZnO / Graphene on Glassy Carbon Electrode in Analysis of Tyrosine. *Int. J. Electrochem. Sci.* **2017**, *12*, 5254–5263. [[CrossRef](#)]
42. Sawkar, R.R.; Patil, V.B.; Shanbhag, M.M.; Shetti, N.P.; Tuwar, S.M.; Aminabhavi, T.M. Detection of ketorolac drug using pencil graphite electrode. *Biomed. Eng. Adv.* **2021**, *2*, 100009. [[CrossRef](#)]
43. Shanbhag, M.M.; Shetti, N.P.; Kalanur, S.S.; Pollet, B.G.; Upadhyaya, K.P.; Ayachit, N.H.; Aminabhavi, T.M. Hf-Doped Tungsten Oxide Nanorods as Electrode Materials for Electrochemical Detection of Paracetamol and Salbutamol. *ACS Appl. Nano Mater.* **2021**, *5*, 1263–1275. [[CrossRef](#)]
44. Shetti, N.P.; Ilager, D.; Malode, S.J.; Monga, D.; Basu, S.; Reddy, K.R. Poly (eriochrome black T) modified electrode for electro-sensing of methdilazine. *Mater. Sci. Semicond. Processing* **2020**, *120*, 105261. [[CrossRef](#)]
45. Chen, C. Physicochemical, Pharmacological and Pharmacokinetic Properties of the Zwitterionic Antihistamines Cetirizine and Levocetirizine. *Curr. Med. Chem.* **2008**, *15*, 2173–2191. [[CrossRef](#)]
46. Gosser, D.K. *Cyclic Voltammetry: Simulation and Analysis of Reaction Mechanisms*; VCH: New York, NY, USA, 1993.
47. Bard, A.J.; Faulkner, L.R. Fundamentals and applications. *Electrochem. Methods* **2001**, *2*, 580–632.
48. Laviron, E. General expression of the linear potential sweep voltammogram in the case of diffusionless electrochemical systems. *J. Electroanal. Chem. Interfacial Electrochem.* **1979**, *101*, 19–28. [[CrossRef](#)]
49. Patil, V.B.; Sawkar, R.R.; Ilager, D.; Shetti, N.P.; Tuwar, S.M.; Aminabhavi, T.M. Glucose-based carbon electrode for trace-level detection of acetaminophen. *Electrochem. Sci. Adv.* **2021**, e202100117. [[CrossRef](#)]
50. Mao, S.; Chen, J. Graphene-based electronic biosensors. *J. Mater. Res.* **2017**, *32*, 2954–2965. [[CrossRef](#)]
51. Tereshchenko, A.; Bechelany, M.; Viter, R.; Khranovskyy, V.; Smyntyna, V.; Starodub, N.; Yakimova, R. Optical biosensors based on ZnO nanostructures: Advantages and perspectives. A review. *Sens. Actuators B* **2016**, *229*, 664–677. [[CrossRef](#)]
52. Patil, R.H.; Hegde, R.N.; Nandibewoor, S.T. Electro-oxidation and determination of antihistamine drug, cetirizine dihydrochloride at glassy carbon electrode modified with multi-walled carbon nanotubes. *Colloids Surf. B Biointerfaces* **2011**, *83*, 133–138. [[CrossRef](#)]
53. GÜngör, S. Electrooxidation of cetirizine dihydrochloride with a glassy carbon electrode. *Die Pharm. Int. J. Pharm. Sci.* **2004**, *59*, 929–933.

54. Karakaya, S.; Dilgin, D.G. Low-cost determination of cetirizine by square wave voltammetry in a disposable electrode. *Mon. Chem. Chem. Mon.* **2019**, *150*, 1003–1010. [[CrossRef](#)]
55. Pourghazi, K.; Khoshhesab, Z.M.; Golpayeganizadeh, A.; Shapouri, M.R.; Afrouzi, H. Spectrophotometric determination of cetirizine and montelukast in prepared formulations. *Int. J. Pharm. Pharm. Sci.* **2011**, *3*, 128–130.
56. Culkova, E.; Lukacova-Chomistekova, Z.; Bellova, R.; Melichercikova, D.; Durdiak, J.; Timko, J.; Rievaj, M.; Tomcik, P. Boron-doped diamond film electrode as voltammetric sensor for cetirizine. *Int. J. Electrochem. Sci.* **2018**, *13*, 6358–6372. [[CrossRef](#)]
57. Mesgari, M.A.; Hamishekar, V.H.; Mohammadnejad, L.; Zakeri-Milani, P. The effects of cetirizine on P-glycoprotein expression and function In vitro and In situ. *Adv. Pharm Bull.* **2016**, *6*, 111–118. [[CrossRef](#)] [[PubMed](#)]
58. Shetti, N.P.; Malode, S.J.; Nayak, D.S.; Bagihalli, G.B.; Kalanur, S.S.; Malladi, R.S.; Reddy, C.V.; Aminabhavi, T.M.; Reddy, K.R. Fabrication of ZnO nanoparticles modified sensor for electrochemical oxidation of methdilazine. *Appl. Surf. Sci.* **2019**, *496*, 143656. [[CrossRef](#)]